Electrostatically functionalized CVD grown multiwalled carbon nanotube/ palladium nanocomposite (MWCNT/Pd) for CH4 detection at room temperature

Prashant Shukla (drprashantdb1980@gmail.com)

Research Article

Keywords: Sensor, Methane, MWCNT, Electrostatic, MOS, Responsivity

Posted Date: April 5th, 2022

DOI: https://doi.org/10.21203/rs.3.rs-1512973/v2

Electrostatically functionalized CVD grown multiwalled carbon nanotube/ palladium nanocomposite (MWCNT/Pd) for CH_4 detection at room temperature

Prashant Shukla [a*], Pooja Saxena [b], Devinder Madhwal [a], Nitin Bhardwaj [a], V.K. Jain [a]
[a] Amity Institute for Advanced Research and Studies (Materials & Devices), Amity University, Sector-125, Noida, 201303, U.P., India
[b] G. L. Bajaj Institute of Technology and Management, Greater Noida, U.P., 201306, India
*Email: drprashantdb1980@gmail.com

ABSTRACT

By reducing the aqueous mixture of electrostatically modified multi-walled carbon nanotubes (f-MWCNT) and palladium (Pd) using $NaBH_4$, a nanocomposite was synthesized. The syllable structure of the f-MWCNT and f-MWCNT/ Pd nanocomposite was investigated by analytical tools FESEM and TEM respectively. f-MWCNTs matrix reinforced with Pd nanoparticles are utilized for sensing
CH_4 with its dilution varying from 0.5-100 ppm in air at room temperature (RT=27°C). The f-MWNT/Pd nanocomposite-based sensor for CH_4 gas show several merits over conventional catalytic beads and MOS based sensors in context of reduced size, reduced power consumption and ease of fabrication. At room temperature, the nanocomposite's temporal electrical responses to CH_4 were measured. It exhibited a response magnitude of ~20-45.71% with a small variation of ±2% towards 0.5-100 ppm CH_4. Furthermore, the responses were extremely reversible and repeatable, implying that it may be used to detect CH_4 at ambient temperature. It has also been demonstrated experimentally that an excellent response time (≈ 20 s) and the recovery time (≈ 25 s) for these devices were recorded for CH_4. The influence of external temperature and humidity on the CH_4 sensor was also investigated in order to assess its long-term stability and self-life. The results showed that very small change is observed over a wide of temperature from 25-70^oC and that for %Rh from 20-90%. Therefore, the reported CH4 sensor absolutely demonstrated long-term stability at ambient conditions and hence, these devices can prove to be ideal for CH_4 leakage detection for practical real time applications. A sensing mechanism by which CH_4 is detected by f-MWCNT/Pd nanocomposite is also elaborately discussed.

Keywords: Sensor, CH_4, MWCNT, Electrostatic, MOS, Responsivity

1. INTRODUCTION

Methane is a colourless, odourless, highly combustible gas found in large quantities in nature. It is generated when natural materials decompose and is found in landfills, marshes, septic systems, sewers, and as a result of a variety of human activities, including coal mining. It's one of the most potent greenhouse gases. Methane is a very stable gas in general, but it is very explosive when mixed with air at a concentration of 5-14%. Coal mines pollute the environment by releasing CH_4 into the atmosphere. Such pollutants have the potential to harm the ecosystem as well as human health **[1]**. As a result, CH_4 monitoring and its remediation is essential to protect public health because it is constantly discharged into the atmosphere.

As a consequence, there is a high necessity for user-friendly and environmentally acceptable sensing systems for on-the-spot, real-time detection of CH_4 emissions, which are extremely hazardous to the environment and human lives. By far, numerous research on CH_4 sensors including MOS gas sensors, photoacoustic-based gas sensor, graphene based gas sensor

and SnO_2-based gas sensor have been published. However, these types of sensors have their own limitations like high power consumption, require continuous Ac supply, poor response and long recovery times etc. [2]. MWCNTs are widely used as sensing material for detection of various gases. The exceptional characteristics of MWCNTs including high aspect ratio, highly sensitive and fast recovery, made it a potential candidate for detection of CH_4 gas at ppm and sub-ppm levels. These characteristics are prerequisites to improve the interaction between CH_4 and MWCNTs. However, pristine MWCNT have a tendency to agglomerate due to their strong sp2 bonding in their hexagonal network. The agglomeration morphology of MWCNT will restrict their efficacy as a gas sensor. Alteration or functionalization of MWCNTs with various functional group is one way to overcome this shortcoming. Moreover, electrical properties of MWCNTs are sensitive towards chemical modifications by functional groups attached onto their surface [3].

Single-walled carbon nanotubes (SWNTs) loaded with palladium (Pd) nanoparticles are used for detection of methane ranging from 6 to 100 ppm in air at room temperature by Lu et al. [4]. For detection of CH_4 leakage in air, Fedorenko et al. **[5]** suggested MOS gas detectors fabricated using Pd/SnO_2 nanoparticles. A sol–gel process was used to make semiconductor detectors based on nanosized Pd-doped tin dioxide. By filling MWCNTs with VO_2, Chimowa et al **[6]** improved CH_4 gas detecting characteristics. MWNTs are filled with vanadium metal and then oxidized using a simple capillary process. At ambient temperature (293 K), the CH4 gas response time improves from 138 s (in V_2O_5) to 16 s (in filled MWNTs), while the recovery times decrease from 234 s to 120 s, respectively. At RT, Janudin et al. **[7]** created a carbon nanotubes-based gas sensor for detecting CH_4 gas. The CNT was functionalized with an amide group and labelled as CNT-amide using the Fischer esterification procedure. Humayun et al. **[8]** demonstrated a highly sensitive, low-cost distributed CH4 sensor system (DMSS) for persistent monitoring, recognition, and detection of CH_4 leaks in natural gas infrastructure such as transmission and distribution pipelines, wells, and production pads. The CH_4 sensing element, a major module of the DMSS, is made up of a metal oxide nanocrystal (MONC) functionalized MWCNT mesh that, when interacting with lower concentrations of CH4, exhibits a higher relative resistance change. Hannon et al. **[9]** used an array of sensors and principal component analysis to address the sensitive detection and discrimination of environmental gases such CH_4, NH_3, SO_2, and CO (PCA). A 32-element chemiresistive array of sensors was constructed using nine different sensor materials, including seven different types of modified SWCNTs and two different polymers. PCA results demonstrate that the chemiresistor sensor chip has excellent discriminating ability in the 1–30 ppm concentration range. Bezdek et al. **[10]** described a chemiresistive sensor made of single-walled carbon nanotubes and a molecular platinum-polyoxometalate complex that is known to mediate CH4 oxidation near ambient conditions. It is demonstrated that the composite is a robust sensor that functions at RT, has air and moisture stability, and CH4 selectivity. The results indicate that techniques from molecular CH4 oxidation can be used to create low-power, low-cost, possibly distributable sensors for selective CH4 detection. Kathirvelan et al. **[11]** used MWCNTs as the sensing element to demonstrate a sensor for detecting and quantifying CH_4. To make the chemiresistive sensor element, silver electrodes were inkjet printed on a glass substrate and then brush coated with MWCNT. The sensor's sensitivity (the increase in resistance caused by analyte exposure) increases linearly with concentration of CH_4, with a maximum sensitivity of roughly 20% recorded for 160 ppm of CH_4. Chakraborty et al. **[12]** demonstrated that sensors based on Fe doped SnO_2 can detect CH4 and butane (primary components of **compressed natural gas and liquified petroleum gas**, respectively) at temperature 350°C. However, at 425°C, the same sensors may detect butane preferentially. Anas et al. **[13]** proposed developing a mine gas detection system composed of gas detecting sensors, a wireless network provider, and a microprocessor. MQ-4 and MQ-7 sensors are used to detect CH_4 and CO, respectively. These sensors are linked to an Arduino board, which is linked to an LCD display that displays

the proportion of CH_4 and CO on a daily basis. Mondal et al. **[14]** investigated the CH4 gas sensing activity of ZnO nano-platelets (average diameter 150–200 nm) synthesized on a Si/SiO_2 substrate using a thermal annealing technique. The sensor response was investigated for various CH_4 gas concentrations (0.1-1%) and operation temperatures ranging from 70-200°C. The ideal temperature range was clearly between 150-200℃, with a sustained magnitude of sensor response as high as 75%. Mishra et al. **[15]** used silver and carbon nanotube films to fabricate and evaluate a surface plasmon resonance-based fibre optic CH4 sensor. The sensor can detect gas concentrations of up to 100 parts per million (ppm).

Most of the commercially available CH_4 sensors are high temperature MOS based sensors require a micro heating element and hence continuous Ac supply for their operation. A versatile, spill-proof, contaminant-free, non-chemical technique based on corona-aided electrostatic charging for modification of MWCNTs has been adopted to attain this critical goal. In this technique, strong electric fields (≈9-13 kV) were used to simultaneously functionalize and deposit MWCNT films in ambient conditions, and the effects of electrostatic corona charging on the characteristics of MWCNT films were examined using various analytical characterization tools. By reducing their aqueous mixture in $NaBH_4$, a nanocomposite of f-MWCNT/Pd was synthesized. In addition, the electrical resistance of the f-MWCNT/Pd nanocomposite films has been carefully examined and characterized in response to their exposure to CH_4 gas concentration. In a sealed test chamber of known volume, the gas sensing properties were investigated at RT under a pressure of 1 atm. The f-MWCNT/Pd nanocomposite films showed excellent CH_4 sensitivity and selectivity, as well as quick response and recovery times.

2. EXPERIMENTAL

2.1. Chemicals & consumables

Chemicals and consumables for cleaning substrates and laboratory glasswares, such as acetone and ethanol etc. were procured from CDH Pvt. Ltd. The Ted Pella industrial grade conductive silver paste was obtained from an electronic component shop in the local market. Navyug Air Products in Noida, India provided the zero-air cylinder utilized in the experiment. For investigations, based on CH_4 detection, a 2 kg canister of CH_4 with a regulator valve is employed.

2.2. Synthesis of the f-MWCNT/Pd nanocomposite

To synthesize functionalized MWCNT (f-MWCNT), CVD grown MWCNT were electrostatically functionalized with high voltage discharge according to a well-defined protocol, followed by its investigation using FT-IR and Raman Spectroscopy to characterize the structural properties of the as-prepared f-MWCNT, which are described in detail elsewhere [12]. By reducing a mixture of f-MWCNTs and Pd salt, the f-MWCNT/Pd nanocomposite was obtained. f-MWNTs (1.0 mg/mL) and palladium chloride (0.75 mg/mL) were typically mixed together in DI water using magnetic stirring. 5 mL of aqueous $NaBH_4$ (0.01 M) solution was added dropwise into 10 mL of the mixture for 30 minutes under ultrasonic treatment to reduce Pd^{2+}.

2.3. Morphological analysis of f-MWCNT/Pd nanocomposite

The surface syllable structure and chemical composition of the sensing f-MWCNT/Pd nanocomposite were examined using a Zeiss scanning electron microscope (SEM) EVO 18. A JEOL JEM 2100 TEM system with a 200 kV accelerating voltage was used for the studies. The microscope is equipped with a beryllium window energy-dispersive (EDS) detector used for HRTEM investigations (Cs = 0.5 mm, point resolution 0.19 nm). Ultrasonically grinding and

dispersing the granular specimens in ethanol for 5 minutes produced the specimens appropriate for TEM analysis. Finally, the particles were carefully put on a copper grid with an amorphous carbon sheet serving as a support.

2.4. Fabrication of the gas sensor electrostatically

The as prepared aqueous dispersion of the f-MWNTs/Pd nanocomposite was ultrasonicated for 2 hours, then centrifuged for 10 minutes at 2000 rpm, the liquid was pipetted off, and the remaining granules were filtered using a glass funnel and filter paper, and then dried at 60°C in a glass petri-dish to produce blackish brown granules that were finely ground before deposition. The corona-aided electrostatic charging was employed to deposit f-MWCNTs/Pd based nanocomposite onto the surface of thin teflon fibres (dia ≈ 250 mm and length ≈ 7-9 mm). The detailed description of the electrostatic corona aided thin film deposition is clearly demonstrated in the supplementary material provide elsewhere **[16]**. Before deposition, a dielectric slurry prepared from a saturated solution of PVAc in acetone was prepared and applied to the surface of teflon fibres to ensure reliable adhesion. The films were then left to dry in the open air for 10-12 hr. A piece of teflon wire with f-MWCNT/Pd nanocomposite coating is soldered to a piece of PCB, and external connections are prepared with Ted Pella industrial grade conductive silver paste. As a consequence, a CH4-gas sensing device based on f-MWNT/Pd nanocomposite coated onto thin teflon wire was developed.

2.5. Experimental setup to measure the sensing response of f-MWCNT/Pd nanocomposite thin films to CH_4

Changes in the electrical conductance of f-MWCNT/Pd nanocomposite thin films when exposed to CH_4 gas in a two-pole configuration under ambient circumstances are used to detect CH4. The gas sensing experiments were carried out in a sealed test chamber with a known volume of 1000 mL at RT and 1 atm pressure. MFCs were utilized to control gas flow and concentration (Digital MFC: Horiba Multi Gas Digital Mass Flow Controller SEC-Z500X and Digital Read Out cum Control Unit PE-D20). The ultra-pure and dry zero air with a humidity percentage < 0.1 % was chosen as the carrier gas for purging CH_4 into the sealed test chamber. The concentration for CH4 was maintained between 0.5-100 parts per million (ppm) (0.0005-0.1 ml per 1000 ml of zero air) using a three-way check valve and a controlled flow rate of zero air at 1000 ml/min. The valves were appropriately regulated and managed, allowing the sensor to be exposed in the closed test chamber to a mixture of clean zero air and CH_4 gas while maintaining a constant pressure and flow rate. Data was taken 5 min after the target gas was put into the test chamber to ensure proper dispersion and mixing of the target gas within the test chamber. The temporal responses of the variation in the electrical resistance of the sensing film was recorded using a computer-aided workstation coupled to a Keithley 6514 high precision electrometer via USB-GPIB interface. The experimental setup used for gas sensing investigations is depicted schematically in Fig. 1. The change in electrical resistance of the sensing film, % S, or sensor response of the f-MWCNT/Pd nanocomposite film to CH_4 gas is calculated using Eq. (1) **[17,18]**.

$$\%S = \left[\frac{R_{Max} - R_0}{R_0}\right] \times 100 \qquad (1)$$

where R_0 (kΩ) is the base value of electrical resistance in air (in absence of CH_4)

R_{Max} (kΩ) is the steady-state electrical resistance value of the sensing film in response to the target gas

Response time τ_{Res}(s) is the time taken by the sensor to reach 90% of its steady-state electrical resistance value

Recovery time, τ_{Rec}(s) is the time taken by the sensor to retrieve back to 90% of its electrical resistance base value, i.e. R_0 (kΩ).
The gas sensing test chamber, as stated above, was flushed with dry zero air before being exposed to target gas to eliminate interfering effects on sensor efficacy caused by environmental humidity.

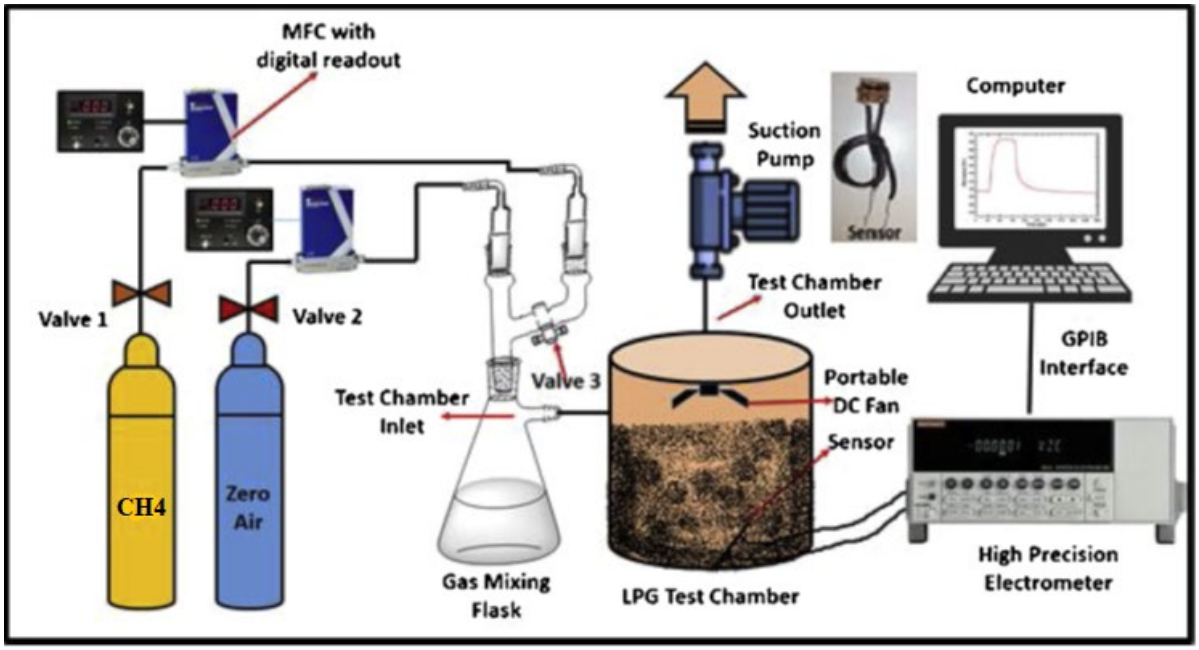

Fig. 1. A pictorial representation of the experimental setup for CH_4 sensing.

3. RESULTS AND DISCUSSIONS

3.1. SEM Micrographs

The field enhanced scanning electron microscope (FESEM) images (Fig. 2) show swirled and bundled morphology of f-MWCNTs. Chemical composition of f-MWCNT was determined applying EDS inside the TEM column to provide insights into the concentration of trace metal impurities. Owing to the vapor phase oxygen modification of the tubes, trace of oxygen can be seen in the EDS spectra. The EDS data shown in the inset of Fig. 2 confirmed the presence of large amounts of Pd nanoparticles on the surface and sidewalls of the MWCNTs. The spectra indicate the presence of significant amount of Pd which is attributed to its uniform dispersion in the f-MWCNT matrix. However, no peak appeared regarding the metal contaminations verifying high purity of the tubes.

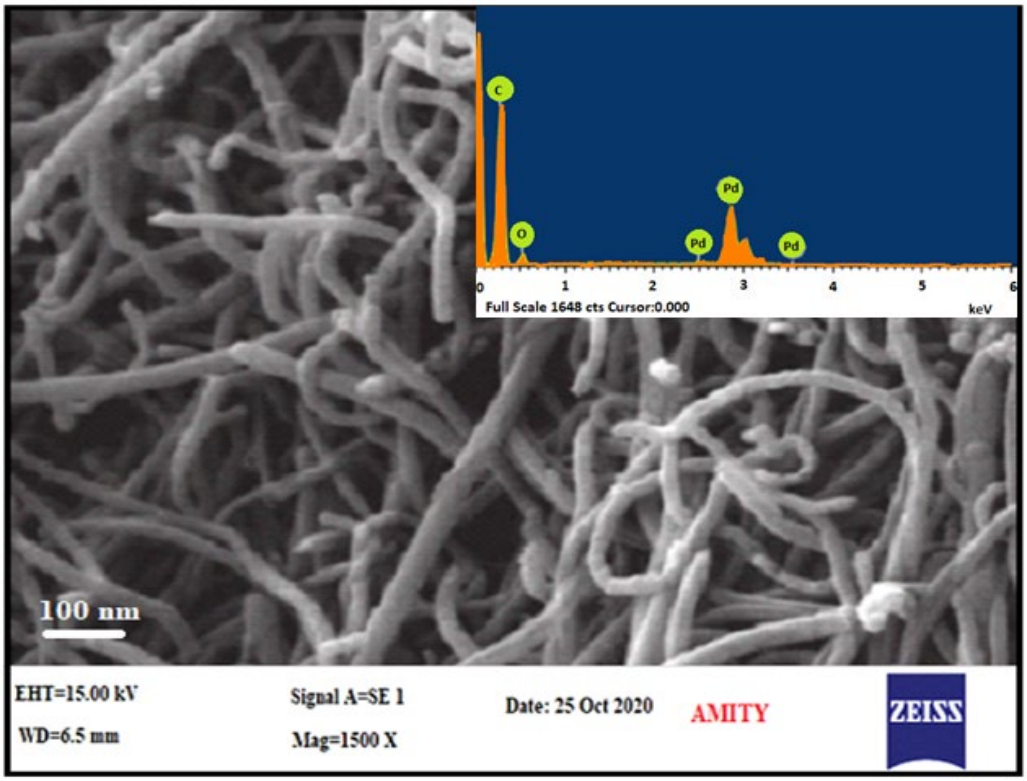

Fig. 2. FESEM image of f-MWCNT and inset shows EDS results for f-MWCNT-Pd nanocomposite

3.2. TEM Micrographs

Fig. 3(a) show the HRTEM micrograph of pristine f-MWNT and Fig. 3(b) show the TEM micrograph of f-MWNT/Pd nanocomposite. Clearly, most of the pristine and purified f-MWCNTs are free from metal contaminations and there are a limited number of defects on the tube sidewalls. In addition, amorphous carbon wrapped around pristine and purified f-MWCNTs. The arrow in Fig. 3(a) highlights the locations of amorphous carbon and sidewall damages in the functionalized tubes. It can be concluded that electrostatic functionalization of MWCNT leads to the removal of amorphous carbon from the tube sidewall and introduce some defects along the MWCNT surface. These defect sites could enhance the susceptibility of the tubes for interacting with other functional groups. The palladium nanoparticles are well disseminated in the f-MWNTs matrix, as can be seen in Fig. 3(b). **Only Pd particles with an average size of 12 nm make up the black dots as confirmed by the EDS analysis of the f-MWCNT-PD nanocomposite.**

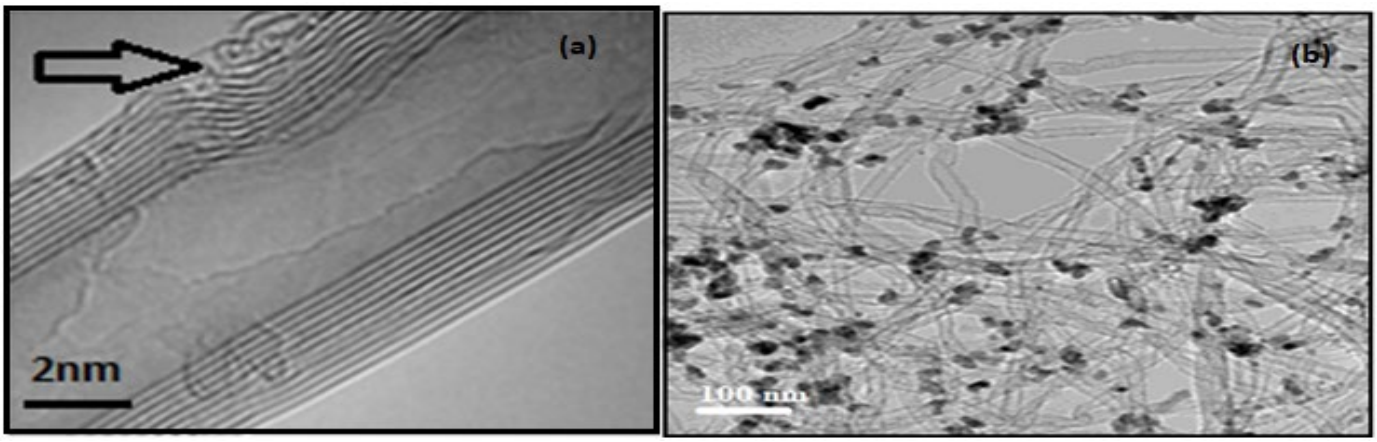

Fig. 3. (a) HRTEM image of f-MWCNT (b) TEM image of f-MWCNT/ Pd nanocomposite

3.3. Electrical measurements of sensor's gas sensing performance

The variation in the electrical conductance of the sensing film with its exposure to CH_4 was observed and temporally plotted to examine the sensor response. The base value of the electrical resistance of f-MWCNTs/ Pd based sensing devices is typically found out to be 35±2 kΩ in zero-air under ambient environmental conditions. All of the electrical observations were conducted at RT and at a pressure of 1 atm.

3.4. Selectivity studies on f-MWCNT/ Pd nanocomposite based sensor

It should be noted that a gas detector must have specificity in addition to high sensitivity in order to be useful for real-time applications. A MWCNTs-based gas sensor can achieve astonishingly high responsivity and specificity by customizing or grafting MWCNTs with a sensitive chemical or molecular group or ion that can promptly sense the target gas. The simplicity with which MWCNTs may be tailored distinguishes them from other materials and sensor development methodologies such as electrochemical sensing, MOS-based sensing, and infrared absorption sensing. The technique is particularly selective and irresponsive to other standard chemical interferents due to the unique interaction and redox reaction among CH_4 gas and f-MWCNTs/ Pd nanocomposite. The gas sensing characteristics of the as-prepared f-MWCNT/Pd sensors were examined at RT by exposing them to a variety of gases at 100 ppm concentration. We studied and compared the sensor responsivity to the gases that are predicted to be major interferents to the CH_4 sensor, as shown in Fig. 4, viz. CO, IPA, NO_2, NH_3, C_2H_5OH, Benzene, Acetone, CO_2, and so on. A maximum sensor response of 45.71 % over all target gases confirms the sensor's outstanding selectivity and sensitivity to CH4 over other vapors and gases. Because of their strong CH_4 selectivity, these sensors did not require scrubbers to remove potential interferents in order to achieve acceptable accuracy. The f-MWCNT/Pd nanocomposite film's selectivity for CH_4 detection is mostly owing to the rolling framework of MWCNTs, which increases the aspect ratio of the sensor and speeds up gaseous adsorption on the sensor surface **[19]**. Furthermore, the presence of many imperfections and impurities, in addition to reactable oxygenation sites attached to the sidewalls of MWCNTs, promotes charge transference between CH_4 molecules and the sensor surface **[20]**. The exceedingly weak interaction of target gases on f-MWCNT sensing surface accounts for the poor sensing response for other gas molecules. **f-MWCNT-Pd nanocomposite show significant response to CH_4. It is possible that the electrostatic treatment might have introduced more number of defects and active oxygenated sites, allowing reasonable sensitivity to the target gases. The presence of oxygenated functionalities at the ends of the f-WCNTs facilitates electron transfer with**

target gases. The larger response with oxygenated carbon nanotubes might be the result of introduction of more controlled hydroxyl groups, which forms low-energy adsorption sites and facilitates charge transfer at defect sites [21]. The change in conductivity resulting from interaction of certain gases with f-MWCNTs has also been ascribed to the formation of hydrogen bond between the functionalized group and the target gas molecule. Second, the introduction of Pd nanoparticles enhanced the catalytic activity of f-MWCNT-Pd nano-composites. Pd as well as other transition metals such as Pt and Ru is often used for catalytic combustion of methane. According to the observations, the RT f-MWCNT sensor is highly specific and responsive to CH_4.

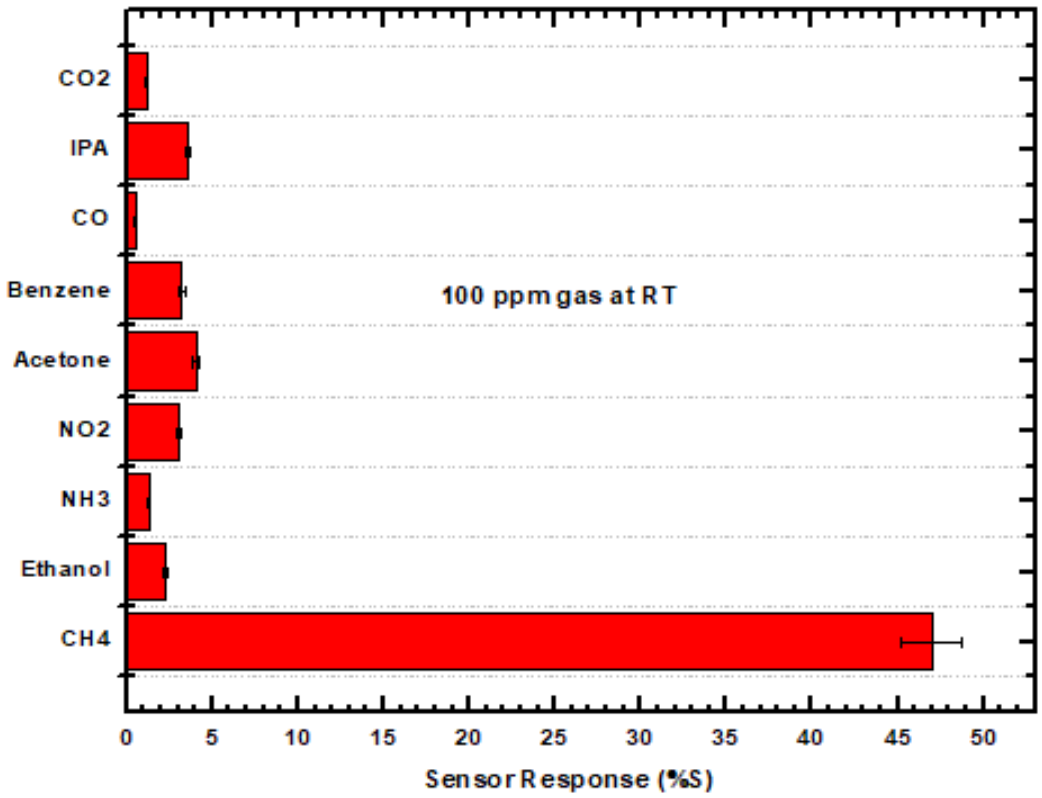

Fig. 4. Selectivity and sensor response of f-MWCNT/Pd nanocomposite-based sensor at RT to various gaseous analytes at 100 ppm.

3.5. Sensitivity & reproducibility studies on CH4 sensor

The sensor's dynamic effectiveness is demonstrated in Fig. 5 by exposing the f-MWCNT/Pd nanocomposite-based sensing film to CH_4 concentrations ranging from 0.5 to 100 ppm at RT. Surprisingly, when exposed to varied ppm levels of CH_4, the sensor displayed great sensitivity. When exposed to CH_4 gas, the electrical resistance of the sensor increases dramatically due to CH_4 molecule absorption on its surface. Similar results were achieved with randomly selected samples throughout multiple test cycles, with just a ±2% variation in sensitivity. It's worth mentioning that, as shown in Fig. 5, the time it takes for the resistance to equilibrate for CH_4 varies between 20-25s depending on the concentration of CH_4 gas. Fig. 6 depicts the percentage increase in electrical resistance of the f-MWCNT/Pd nanocomposite film as a function of CH_4 concentration. As the CH_4 concentration grows from 0.5-100 ppm, the electrical resistance of the sensor film rises from 20 to 45.71%. This demonstrated a significant boost in system responsiveness as compared to commercially available MOS-based CH_4 detectors. As

demonstrated in Fig. 5, forceful flushing of dry zero air is utilized to expel and banish chemi-assimilated CH_4 residues from the surface of the f-MWCNT/Pd nanocomposite film, causing its electrical conductance to recover to near-base value. As a result, it is repeatable and reusable.

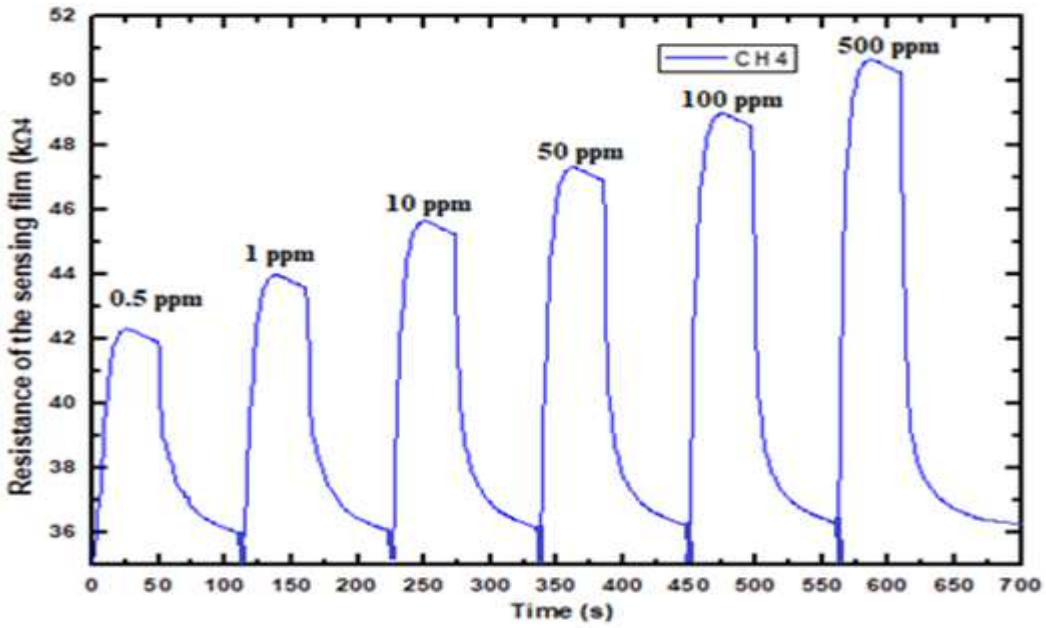

Fig. 5. Temporal response of the sensor when exposed to different ppm levels of CH_4 at RT and 1 atm pressure.

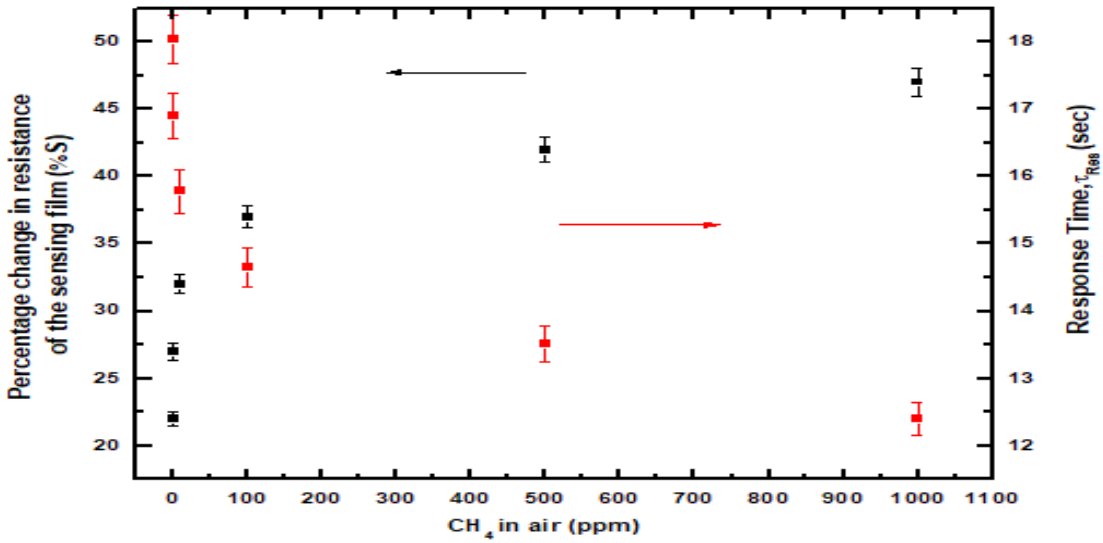

Fig. 6. The percentage responsivity (%S) and the sensor response time, *τRes* (sec) for CH_4 sensor is plotted against different concentrations varying from 0.5-1000 ppm. The error bars represent ±2% change.

3.3.3. Stability and self-life investigations on CH_4 sensor

Periodic inspection for 30 days was used to assess the stability and shelf-life of the present CH_4 sensor. Throughout the testing time, the sensor was constantly exposed to the ambient environment. As shown in Fig. 7, typical response curves of a sensing test to demonstrate the

sensor's inherent stability characteristic for 100 ppm CH_4 at RT were performed over 30 days, demonstrating the sensor's long-term stability and self-life. The dynamic response of the sensor is illustrated in the inset of Fig. 7, with no notable change in response and recovery rates between day 1 and day 30. The fabricated f-MWCNT/Pd nanocomposite sensor's high-performance CH4 detecting characteristics provide cutting-edge technology for toxic CH_4 gas in the mining, home, and commercial sectors.

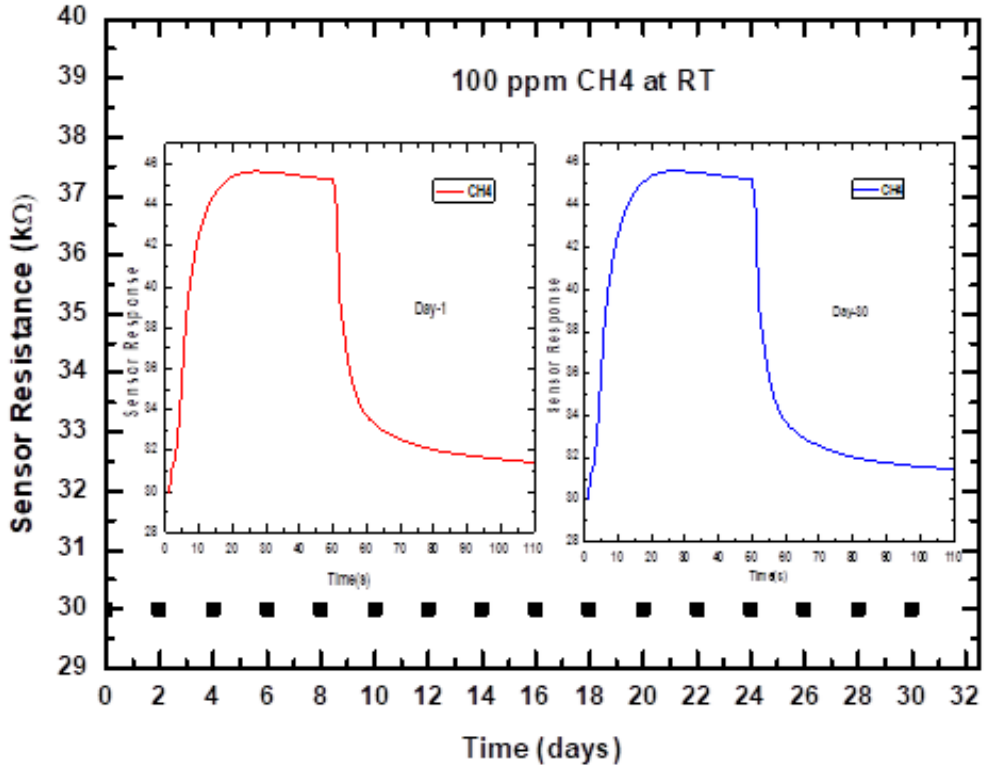

Fig. 7. Typical response curves for 100 ppm METHANE at RT performed on the same sensor over 30 days.

3.3.4. Humidity and temperature tolerance studies on CH_4 sensor

The two key concerns for different gas and chemical sensors, namely electrochemical sensors, MOS-based sensors, IR-based sensors, and colorimetric sensors, are environmental humidity and temperature. Our sensor's humidity and temperature-dependent tolerance has been thoroughly examined. Although the humidity and temperature of the surrounding environment have a substantial impact on sensor performance, this is a well-known but correctable issue. The sensor responsivity for 100 ppm of CH_4 was monitored and investigated for relative humidity (%RH) in the range 35-90% at RT and operating temperature range 30-75°C for real time practical applications. The temperature and pressure of the system also have an effect on the %RH. The interferent to sensor performance under consideration in this study is % RH, and the temperature was held constant for a proper assessment. The ambient humidity and temperature were measured using a commercial Acurite Pro Accuracy Indoor Humidity & Temperature Monitor with a sensitive probe. All experiments were carried out in a digital microprocessor-controlled humidity chamber (REMI SC-10 Plus) with precisely regulated temperature and humidity controls and a dual display PID microprocessor-controlled double walled thermally insulated oven with electrical feedthrough to investigate the effects of humidity and temperature on f-MWCNT/Pd nanocomposite-based CH_4 sensor. To lower the % RH below the ambient level, silica gel was used. Environmental dampness, on the other hand, has a major impact on

sensor performance. In the practical humidity range of 35-65 %RH, a relatively steady sensor response with a variance of roughly 0.001% for CH_4 was measured, as shown in Fig. 8. Although carbon nanotubes contain both electrons and holes, they are most typically considered as a p-type semiconductor **[22]**. Because CNTs are **hydrophilic**, they interact with water molecules on a microscopic level **[23]**. Surface functional groups such as -OH or -COOH are formed as a result of the adsorption of H_2O molecules on the surface of CNTs. Because the p-bonds between nanotube walls are sp2 hybridised, water molecules adsorb on the surfaces of CNTs or between CNT walls, with electric charge transference recognized as a chemical process. H_2O molecules are adsorbed on CNT surfaces when exposed to dampness. The amount of adsorption is determined by the %RH. Because of the shift in electrical potential, electrons transfer from H_2O molecules to CNTs during adsorption. Rising humidity, as seen in Fig. 8, raises the electrical resistance of the sensor, which continues until the % RH reaches 70-80 %. Electrons migrating from H_2O molecules to CNTs recombine with majority carriers (holes) in CNTs, reducing the availability of holes in CNTs and hence decreasing the electrical conductance of the sensor. H_2O molecules have a critical role to play in electron donation. The sensor's electrical resistance's inclination to decrease with rising humidity over a particular %RH can be linked to two mechanisms: To begin with, the number of electron carriers increases as the quantity of electron impurity in CNTs increases. At higher RH levels, electrons become the predominant carriers in CNTs, transforming them from p-type to n-type. As the amount of adsorption generated electrons grows, the electrical resistance of the sensor decreases. Finally, when humidity rises, a conducting electrolytic layer forms on the surface of the nanotube. The overall resistance of the sensor is reduced since this resistor is used in parallel with the CNT resistor. The Fermi level shift and the depletion layer width grows as a result of charge carrier transfer. Aside from charge carrier transference, two other factors may impact the electrical resistance of the sensor: the chemical interaction of hydrogen (-H+ group) with CNT surface oxygen (owing to surface impurities) and the change in nanotube distance **[24]**. The sensor's sensitivity to humidity, on the other hand, should not interfere with its ability to detect target gases, because surface absorption of the target gas in the presence of dampness would change its resistance value further in comparison to the prior base resistance value. This problem is readily solved by exposing it just to ambient humidity and avoiding other detectable gaseous analytes by utilizing another sensor with identical physical, chemical, and electrical properties as a reference sensor and building the detecting device as an electronic gadget.

Experiments were also carried out with 100 ppm CH_4 at various temperatures above RT ranging from 30-75°C to evaluate the effect of temperature on sensor responsiveness to CH_4. The influence of temperature on the sensing device is seen in the inset of Fig. 8. The sensor response becomes virtually constant as the temperature rises to 65°C. The resistance of the sensing film increased as the temperature increases, resulting in an increase in sensor response. The rate of change in resistance per degree increase in temperature, on the other hand, is just 10.2/°C. This implies that the sensors are particularly temperature sensitive. Beyond 65°C (beyond the operable temperature range), there is a rapid rise in resistance and hence sensor response, which is produced by the desorption of ambient humidity from the proximity of the sensor device, as temperature and humidity are inversely related.

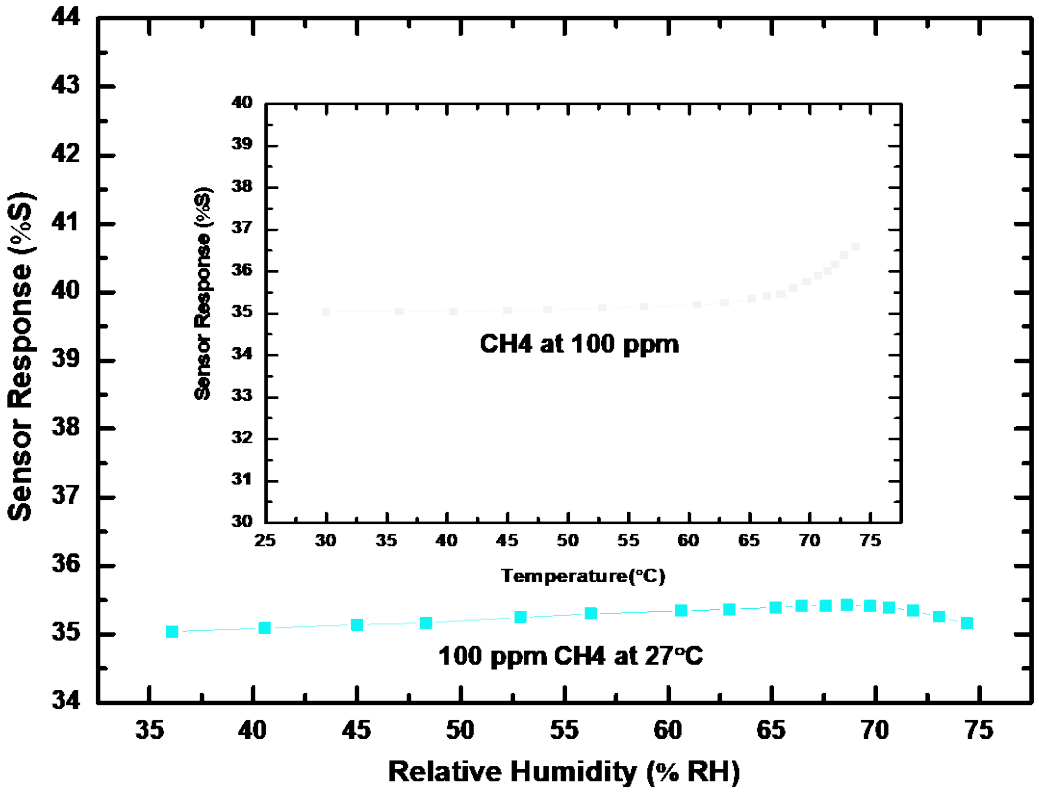

Fig. 8. Sensor response (%S): with respect to relative humidity (%RH) and in the inset with respect to temperature (°C).

3.3.3. Methane sensing mechanism

The electrostatic corona charging approach was used not only to functionalize MWCNTs, but also to generate and attach highly reactive oxygenated sites on f-MWCNTS/Pd nanocomposite thin film **[25]**. The high temperature created by electrostatic corona agitation ionizes the gas molecules in the film's proximity. As a result, it is thought that during electrostatic corona charging, ambient oxygen, the most common oxidizing gas, was ionized to native oxygen and adsorbed onto the surfaces of f-MWCNT/Pd nanocomposite. It is widely known that p-type MWCNT-based gas sensors are very common **[26,27]**. Under ideal environmental conditions, f-MWCNT has a p-type character due to the electron sensitive nature of absorbed moisture or oxygen moieties. When semiconducting p type MWCNTs are exposed to the ambient air, oxygen molecules are adsorbed on their surfaces as per Eq. 1, removing electrons from the MWCNTs' conduction band and generating an electron depletion layer in the surface area, according to Kazemi et al. **[28]**. As shown in Eq (2) and (3), at low temperatures, O_2 absorbs one electron from the MWCNT surface, but at high temperatures, O_2 absorbs two electrons from the MWCNT surface. Desorbed oxygen molecules occur when adsorbing oxygen molecules interact with target gas molecules. Native oxygen is adsorbed on the surface of MWCNTs, resulting in active oxygenated bond forming sites. MWCNTs will be adsorbed with water molecules from their surroundings, resulting in observable electron donor activity. The described active oxygenation sites are more likely to interact with ambient moisture moieties, resulting in hydroxyl groups as functional or activated sites.

According to Arai et al. **[29]**, based on the processes shown in Eq (5)-(7), non-dissociative and dissociative adsorption schemes may prevail:

$$O_{2(gas)} \leftrightarrow O_{2(adsorbed)} \quad (1)$$

$$O_{2(gas)} + e^-_{(surface)} \leftrightarrow O^-_{2(adsorbed)} \quad (2)$$

$$O_{2(gas)} + 2e^-_{(surface)} \leftrightarrow 2O^-_{(adsorbed)}$$

OR (3)

$$O^-_{2(adsorbed)} + e^-_{(surface)} \leftrightarrow 2O^-_{(adsorbed)}$$

$$O^-_{(adsorbed)} + e^- \leftrightarrow O^{2-}_{(adsorbed)} \quad (4)$$

$$H_2O(g) \rightarrow H_2O^+(\text{ad}) + e^- \quad (5)$$

$$H_2O(g) + O_o^{2-} + V_o^- \rightarrow 2OH_o^-(ad) + e^- \quad (6)$$

$$H_2O(g) + O_o^{2-} + V_o^{2-} \rightarrow 2OH_o^-(ad) + 2e^- \quad (7)$$

Where V_o^- *and* V_o^{2-} *are oxygen vacant sites trapping one or two electrons*

The MWCNT-based resistive gas sensor's detection approach is based on changes in the electrical resistance of the MWCNT matrix, which is altered by target gas molecule adsorption-desorption through charge transfer processes. In summary, target gas adsorption on the MWCNT surface can change the electrical resistance by altering the Schottky barrier at the electrode-MWCNT junction, charge transfer between MWCNT and target analytes, and the MWCNT intratubular junction distance **[30]**. In ambient conditions, MWCNTs obviously act as a p-type semiconductor. The drop in hole concentration generated by electron migration into the valence band of MWCNTs as a result of target analyte assimilation increases resistance. On the contrary, when electrons are removed from p-type MWCNTs, they enhance hole concentration while lowering resistance. The increased charge ability in MWCNTs generated by the inclusion of scattering sites is also responsible for the change in electrical resistance. Resistance may change if target analytes are adsorbed on the MWCNT-metal interface due to variances in the Schottky barrier. Because a single MWCNT is inadequate to construct a conducting route, the conducting path is often formed by connecting many MWCNTs. If the analytes are adsorbed on the intertube junction, modifying the inter-tubular junctions can also affect MWCNT resistance. The presence of four σ bonds in the CH_4 molecule makes it totally stable and prohibits it from interacting with other molecules via bonding and non-bonding orbitals. High specific area MWNTs are suitable for CH_4 adsorption. However, there is no charge transfer between the inert CH_4 and the MWNTs, resulting in no change in electrical characteristics. As a result, it was observed that pure MWNTs are CH_4 insensitive. The Pd applied to the f-MWNTs in the composite has a significant influence on the CH_4 reactivity of the nanocomposite.

When the f-MWCNT/Pd nanocomposite surface is exposed to reducing gas like methane that works as an electron donor, the gas reacts with the chemisorbed oxygen thereby releasing electrons back to the conduction band. The overall reducing reactions between CH_4 gas, and the chemisorbed oxygen species (O^- and O^{2-}) are indicated in reaction pathways in Eqs. (8) and (9) as explained by Wetchakun et al. **[1]**. Methane desorbs chemically adsorbed oxygen ions and physically adsorbed hydroxyl ions from the f-MWCNT/Pd nanocomposite surface during this interaction but enriches it with electrons owing to the oxidation process.

$$CH_4 + 4O^-(ads) \rightarrow 2H_2O + CO_2 + 4e^- \quad (8)$$

$$CH_4 + 4O^{2-}(ads) \rightarrow 2H_2O + CO_2 + 8e^- \quad (9)$$

Furthermore, we compared the CH_4 sensing performances of the presently developed CH_4 sensor and the previously reported sensors based on variety of nanostructures and nanohybrids, which are summarized in Table 1. It was noticed that the presently developed sensor showed higher responses compared to most of the reported room temperature CH_4 sensors, even higher or comparable to some sensors working at high temperatures. Moreover, our sensor was particularly attractive for its fast response and recovery rate as well as excellent sensitivity and reversibility at room temperature.

Table 1
Comparison of room-temperature CH_4sensing performancesbetween the presently developed sensor and reported CH_4 sensors based on various nanostructures and nanohybrids. **[31]**

Sensitive material	CH_4 (ppm)	Temperature	R	Response/recovery time	Ref.
MWCNT/Pd	20000	R.T.	7%	310 s/176 s	[32]
Au/VO_x films	1000	R.T.	22%	~800 s/~800 s	[33]
VO_2	500	R.T.	3.2%	Not reported	[34]
PbS nanocrystals	50000	R.T.	47.6%	Not reported	[35]
Pd-doped SnO_2/rGO	12000	R.T.	9.5%	5 min/7 min	[36]
rGO/SnO_2	10000	R.T.	76%	ca. 150 s/150 s	[37]
NiO/rGO	1000	R.T.	~1.0%	Not reported	[38]
Graphene/PANI	3200	R.T.	5%	85 s/45 s	[39]
SnO_2@rGO	10000	150 °C	76.3%	30 s/800 s	[40]
Graphene/SnO_2	10000	150 °C	~50%	ca. 200 s/200 s	[41]
ZnO/rGO	4000	190 °C	4.5%	200 s/200 s	[42]
f-MWCNT/Pd	0.5	R.T.	45.71%	20s/ 25s	This work

As a result, the concentration of electrons on the surface of f-MWCNT/Pd nanocomposite increases and the resistance of n-type MWCNT layer decreases. In contrast, the resistance of p-type MWCNT surface increases because generated electrons recombine with holes, decreasing in the hole concentration and increasing the sensor's resistance depending on the concentration availability of the target gas, CH_4 as shown in Fig. 9. On the contrary, similar figure for CNTs/SnO_2 nanoparticles was reported by Dehghani et al **[43]**.

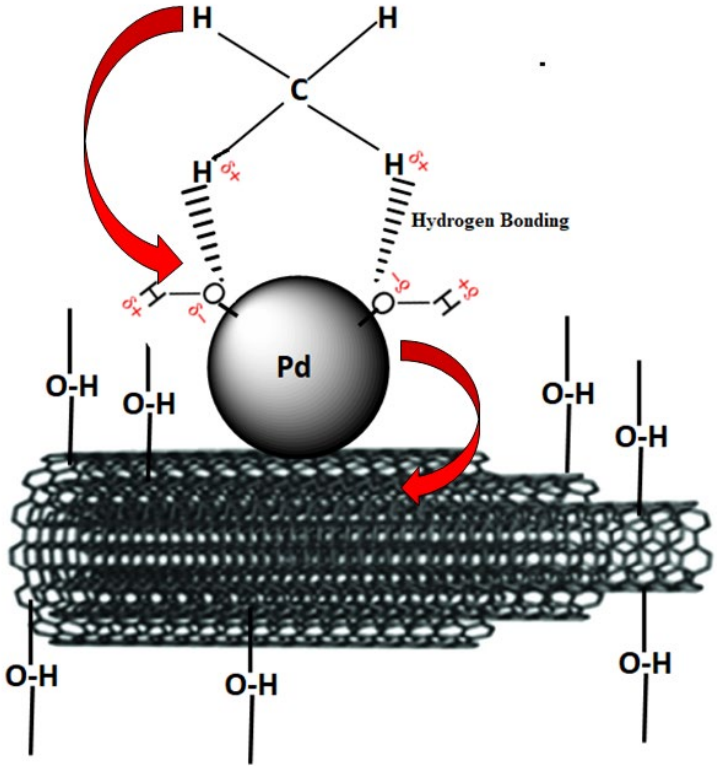

Fig. 9. Proposed sensing mechanism for CH_4 detection using f-MWCNT/ Pd sensor at RT

4. CONCLUSION

Finally, we demonstrated the sensing performance of an electrostatically functionalized and deposited MWCNT/Pd nanocomposite film on a suitable substrate for a highly sensitive, selective, reproducible, and reusable sensing system for detection of traces of the highly toxic and hazardous gaseous analyte CH_4 in air at ambient temperature and pressure conditions. The gas detection device may be reused numerous times simply by blowing away the adsorbed CH_4 species under atmospheric conditions with zero air. It was discovered that the corona assisted electrostatic self-assembly thin film patterning technique for batch fabrication of gas sensors is quick, simple, low-cost, and conforms to sensor fabrication on large areas of the substrate that can be lithographically patterned to produce an array of sensors. This technique has the potential to be employed in lab-on-a-chip applications, wearable sensors, and other small portable electronic device applications.

Acknowledgements

Authors thank Dr. Ashok K. Chauhan, founder president, Amity University, for his continuous support and encouragement. Authors would also like to thank other members of the AIARS (M&D) group, Amity University, Noida for their support.

CRediT authorship contribution statement

Prashant Shukla: Methodology, Investigation, Conceptualization, Visualization, Writing - original draft. **Pooja Saxena:** Validation, Graphics Designing, Writing - review & editing. **Devinder Madhwal:** Prototype development, Writing - review & editing. **Nitin Bhardwaj:** Experimental Investigation, Set Up Establishment. **V.K. Jain:** Supervision, Writing - review & editing.

Declaration of Competing Interest

The Authors declares that there is no conflict of interest. All authors have approved the manuscript and agree with submission to your esteemed journal.

Data Availability Statement

The data that support the findings of this study are available from the corresponding author upon reasonable request.

References

1. **K. Wetchakun, T. Samerjai, N. Tamaekong, C. Liewhiran, C. Siriwong, V. Kruefu, A. Wisitsoraat, A. Tuantranont, S. Phanichphant, Semiconducting metal oxides as sensors for environmentally hazardous gases, Sensors and Actuators B: Chemical, 160(1) 580 (2011). DOI: https://doi.org/10.1016/j.snb.2011.08.032.**
2. **R.K. Roy, M. Pal Chowdhury, A.K. Pal, Room temperature sensor based on carbon nanotubes and nanofibres for methane detection, Vacuum, 77(3) 223 (2005), DOI: https://doi.org/10.1016/j.vacuum.2004.08.023.**
3. **Yang Li, Huicai Wang, Yousi Chen, Mujie Yang, A multi-walled carbon nanotube/palladium nanocomposite prepared by a facile method for the detection**

of methane at room temperature, Sensors and Actuators B: Chemical, 132(1) 155 (2008). DOI: https://doi.org/10.1016/j.snb.2008.01.034.

4. **Yijiang Lu, Jing Li, Jie Han, H.-T. Ng, Christie Binder, Christina Partridge, M. Meyyappan, Room temperature methane detection using palladium loaded single-walled carbon nanotube sensors, Chemical Physics Letters, 391(4-6) 344 (2004). DOI: https://doi.org/10.1016/j.cplett.2004.05.029.**
5. G. Fedorenko, L. Oleksenko, N. Maksymovych, Galina Skolyar, Oleksandr Ripko, Semiconductor Gas Sensors Based on Pd/SnO_2 Nanomaterials for Methane Detection in Air. Nanoscale Research Letters **12,** 329 (2017). DOI: https://doi.org/10.1186/s11671-017-2102-0
6. George Chimowa, Zamaswazi P. Tshabalala, Amos A. Akande, George Bepete, Bonex Mwakikunga, Suprakas S. Ray, Evans M. Benecha, Improving CH_4 gas sensing properties of multi-walled carbon nanotubes by vanadium oxide filling, Sensors and Actuators B: Chemical, **247,** 11 (2017). DOI: https://doi.org/10.1016/j.snb.2017.02.167.
7. Nurjahirah Janudina, Norli Abdullahb, Faizah Md Yasinc, Mohd Hanif Yaacobd, Muhammad Zamharir Ahmade, Luqman Chuah Abdullahc, Raja Nor Izawati Raja Othmanf, Noor Aisyah Ahmad Syahb, Shafreeza Sobric, Noor Azilah Mohd Kasimb, Carbon Nanotubes-based Gas Sensor in Detection of Methane Gas at Room Temperature, ZULFAQAR International Journal of Defence Science, Engineering & Technology, **1(2),** 76 (2018).
8. Md Tanim Humayun, Ralu Divan, Liliana Stan, Daniel Rosenmann, David Gosztola, Lara Gundel, Paul A. Solomon, Igor Paprotny, Ubiquitous Low-Cost Functionalized Multi-Walled Carbon Nanotube Sensors for Distributed Methane Leak Detection, IEEE Sensors Journal, **16(24),** 8692 (2016). DOI: https://doi.org/10.1109/JSEN.2016.2581832.
9. A. Hannon, Y. Lu, J. Li, M. Meyyappan, A Sensor Array for the Detection and Discrimination of Methane and Other Environmental Pollutant Gases. Sensors (Basel) **16(8)** 1163 (2016). DOI: https://doi.org/10.3390/s16081163.
10. Máté J. Bezdek, Shao-Xiong Lennon Luo, Kang Hee Ku, Timothy M. Swager, A chemiresistive CH_4 sensor, Proceedings of the National Academy of Sciences **118 (2),** e2022515118 (2021). DOI: https://doi.org/10.1073/pnas.2022515118.
11. J. Kathirvelan, R. Vijayaraghavan, Detection of CH_4 using multi-walled carbon nanotubes, Bulletin of Material Science, 38(4) 909 (2015). DOI: https://doi.org/10.1007/s12034-015-0940-x.

12. S. Chakraborty, A. Sen, H.S. Maiti, Selective detection of CH_4 and butane by temperature modulation in iron doped tin oxide sensors, Sensors and Actuators B: Chemical, **115(2)** 610 (2006). DOI: http://dx.doi.org/10.1016/j.snb.2005.10.046.
13. Mohd Anas, Syed Mohd Haider, Prateek Sharma, Monitoring and Testing in Underground Mines using Wireless Technology, International Journal of Engineering Research & Technology, **6(1)** IJERTV6IS010306 (2017). DOI: http://dx.doi.org/10.17577/IJERTV6IS010306.
14. B. Mondal, J. Dutta, C. Roychaudhury, D. Mohanta, H. Saha, Zinc Oxide Nano-Platelets for Effective Methane Gas-Sensing Applications, Chinese Journal of Physics, **51(5)** 994 **(**2013). DOI: http://dx.doi.org/10.6122/CJP.51.994.
15. S. K. Mishra, S. N. Tripthi, V. Chaudhary, B. D. Gupta, Fiber Optic Methane Sensor Utilizing Ag/CNT Thin Films, *Frontiers in Optics,* OSA Technical Digest (online) (Optical Society of America, 2014), paper FTu2B.3, 2014. DOI: https://doi.org/10.1364/FIO.2014.FTu2B.3.
16. Vasuda Bhatia, Vikesh Gaur, Vinod K. Jain, New technique to deposit thin films of carbon nanotubes based on electrostatic charge deposition and their application for alcohol detection, International Journal of Nanoscience, **8(4)** 443 (2009). DOI: https://doi.org/10.1142/S0219581X09006298.
17. P. Shukla, V. Bhatia, V. Gaur, V.K. Jain, Electrostatically Functionalized Multiwalled Carbon Nanotube/PMMA Composite Thin Films for Organic Vapor Detection, Polymer-Plastics Technology and Engineering, **50 (11)** 1179 (2011). DOI: https://doi.org/10.1080/03602559.2011.574668.
18. S. Ahlersa, G. Muller, T. Dollb, A rate equation approach to the gas sensitivity of thin film metal oxide materials, Sensor and Actuator B: Chemical **107(2)** (2005) 587. DOI: https://doi.org/10.1016/j.snb.2004.11.020.
19. J. Tian, G. Yang, D. Jiang, F. Su, Z. Zhang, A hybrid material consisting of bulk-reduced TiO_2, graphene oxide and polyaniline for resistance based sensing of gaseous ammonia at room temperature, Microchimica Acta, 183 2871 (2016). DOI: https://doi.org/10.1007/s00604-016-1912-6.
20. T.A.J. Siddiqui, B.G. Ghule, S. Shaikh, P.V. Shinde, K.C. Gunturu, P.K. Zubaidha, J.M. Yun, C. O' Dwyer, R.S. Mane, K.H. Kim, Metal-free heterogeneous and mesoporous biogenic graphene-oxide nanoparticle-catalyzed synthesis of bioactive benzylpyrazolyl coumarin derivatives, RSC Advances, **8 (31)** 17373 (2018). DOI: https://doi.org/10.1039/C7RA12550J.

21. Nguyen H., Huh J. Behavior of Single-Walled Carbon Nanotube-Based Gas Sensors at Various Temperatures of Treatment and Operation. Sensor and Actuator B: Chemical **117** 426 (2006). DOI: https://doi.org.10.1016/j.snb.2005.11.056.
22. M. Matsumoto, Y. Saito, C. Park, T. Fukushima, T. Aida, Ultrahigh-throughput exfoliation of graphite into pristine 'single-layer' graphene using microwaves and molecularly engineered ionic liquids, Nature Chemistry **7** 730 (2015) DOI: https://doi.org/10.1038/nchem.2315.
23. Ziyu Zhou, Tongchuan Gao, Sean McCarthy, Andrew Kozbial, Susheng Tan, David Pekker, Lei Li, Paul W. Leu, Parahydrophobicity and stick-slip wetting dynamics of vertically aligned carbon nanotube forests, Carbon, **152**, 474, (2019). DOI: https://doi.org/10.1016/j.carbon.2019.06.012.20.
24. Kum-Pyo Yoo, Lee-Taek Lim, Nam-Ki Min, Myung Jin Lee, Chul Jin Lee, Chan-Won Park, Novel resistive-type humidity sensor based on multiwall carbon nanotube/polyimide composite films, Sensors and Actuators B: Chemical, **145(1)**, 120 (2010). DOI: https://doi.org/10.1016/j.snb.2009.11.041.
25. V. K. Jain, V. Bhatia and V. Gaur, Applied for Indian Patent, Dwarka, New Delhi (2008).
26. M. Penza, G. Cassano, R. Rossi, A. Rizzo, M.A. Signore, M. Alvisi, Effect of growth catalysts on gas sensitivity in carbon nanotube film based chemiresistive sensors Applied Physics Letters, **90** 103101 (2007). DOI: https://doi.org/10.1063/1.2456258
27. W.S. Cho, S.I. Moon, K.K. Paek, Y.H. Lee, J.H. Park, B.K. Ju, Patterned multiwall carbon nanotube films as materials of NO2 gas sensors, Sensors and Actuators B: Chemical, **119(1)** 180 (2006). DOI: https://doi.org/10.1016/j.snb.2005.12.004.
28. Kazemi Nader, Hashemi Babak, Mirzaei Ali, Promotional effects of nitric acid treatment on CO sensing properties of SnO2/ MWCNT nanocomposites, Processing and Application of Ceramics **10 (2)**, 97 (2016). DOI: http://dx.doi.org/10.2298/PAC1602097K.
29. H. Arai, T. Seiyama, in: W. G€opel, J. Hesse, J.M. Zemel (Eds.), Sensors: A Comprehensive Survey, vol. 3, VCH Verlag, Weinheim, 1992.
30. Ruixian Tang, Yongji Shi, Zhongyu Hou, Liangming Wei, Carbon Nanotube-Based Chemiresistive Sensors, Sensors **17 (4)** (2017) 882. DOI: https://doi.org/10.3390/s17040882.
31. Yi Xia, Jing Wang, Lei Xu, Xian Li, Shaojun Huang, A room-temperature methane sensor based on Pd-decorated ZnO/rGO hybrids enhanced by visible light

photocatalysis, Sensors and Actuators B: Chemical, **304** 127334 (2020). DOI: https://doi.org/10.1016/j.snb.2019.127334.

32. Y. Li, H. Wang, Y. Chen, M. Yang, A multi-walled carbon nanotube/palladium nanocomposite prepared by a facile method for the detection of methane at room temperature, Sensors and Actuators B: Chemical, **132** 155 (2008). DOI: https://doi.org/10.1016/j.snb.2008.01.034.
33. J. Liang, J. Liu, N. Li, W. Li, Magnetron sputtered Au-decorated vanadium oxides composite thin films for methane-sensing properties at room temperature, Journal of Alloys and Compound, **671** 283 (2016). DOI: https://doi.org/10.1016/j.jallcom.2016.02.003.
34. A.K. Prasad, S. Amirthapandian, S. Dhara, S. Dash, N. Murali, A.K. Tyagi, Novel single phase vanadium dioxide nanostructured films for methane sensing near room temperature, Sensors and Actuators B: Chemical, **191** 252 (2014). DOI: https://doi.org/10.1016/j.snb.2013.09.102.
35. A. Mosahebfard, H.D. Jahromi, M.H. Sheikhi, Highly Sensitive, Room temperature methanegas sensor based on lead sulfidecolloidal nanocrystals, IEEE Sensors Journal, **16** 4174 (2016). DOI: https://doi.org/10.1109/JSEN.2016.2546966.
36. S. Nasresfahani, M.H. Sheikhi, M. Tohidi, A. Zarifkar, Methane gas sensing properties of Pd-doped SnO2/reduced graphene oxide synthesized by a facile hydrothermal route, Materials Research Bulletin, **89** 161 (2017). DOI: https://doi.org/10.1016/j.materresbull.2017.01.032.
37. K.C. Lam, B. Huang, S.Q. Shi, Room-temperature methane gas sensing properties based on in situ reduced graphene oxide incorporated with tin dioxide, Journal of Materials Chemistry A, **5** 11131 (2017). DOI: https://doi.org/10.1039/C7TA01293D.
38. D. Zhang, H. Chang, P. Li, R. Liu, Characterization of nickel oxide decorated-reduced graphene oxide nanocomposite and its sensing properties toward methane gas detection, Journal of Materials Science: Materials in Electronics, **27** 3723 (2016). DOI: https://link.springer.com/article/10.1007/s10854-015-4214-6.
39. Z. Wu, X. Chen, S. Zhu, Z. Zhou, Y. Yao, W. Quan, B. Liu, Room temperature methane sensor based on graphene nanosheets/polyaniline nanocomposite thin film, IEEE Sensors Journal **13** 777 (2013). DOI: https://doi.org/10.1109/JSEN.2012.2227597.
40. S. Sarina, H.-Y. Zhu, Q. Xiao, E. Jaatinen, J. Jia, Y. Huang, Z. Zheng, H. Wu, Viable photocatalysts under solar-spectrum irradiation: nonplasmonic metal nanoparticles,

Angewandte Chemie International Edition **53** 2935 (2014). DOI: https://doi.org/10.1002/anie.201308145.

41. M. Kooti, S. Keshtkar, M. Askarieh, A. Rashidi, Progress toward a novel methane gas sensor based on SnO2 nanorods-nanoporous graphene hybrid, Sensors and Actuators B: Chemical, **281** 96 (2019). DOI: https://doi.org/10.1016/j.snb.2018.10.032.
42. D. Zhang, N. Yin, B. Xia, Facile fabrication of ZnO nanocrystalline-modified graphene hybrid nanocomposite toward methane gas sensing application, Journal of Materials Science: Materials in Electronics, **26** 5937 (2015). DOI: http://dx.doi.org/10.1007/s10854-015-3165-2.
43. S. Dehghani, M. Mohammadzadeh, M.H. Sheikhi, M.K. Moravvej-Farshi, Room temperature methane sensor based on single wall CNTs/SnO_2 nanoparticles. Micro Nano Letters, **14** 815 (2019). DOI: https://doi.org/10.1049/mnl.2018.5417.